Bull. Astr. Soc. India (2010) **38**, 103–112

Further GMRT observations of the Lockman Hole at 610 MHz

T. S. Garn,[1*] D. A. Green,[2†] J. M. Riley[2] and P. Alexander[2,3]
[1]*SUPA, Institute for Astronomy, Royal Observatory of Edinburgh, Blackford Hill, Edinburgh EH9 3HJ, United Kingdom*
[2]*Astrophysics Group, Cavendish Laboratory, 19 J. J. Thomson Avenue, Cambridge CB3 0HE, United Kingdom*
[3]*Kavli Institute for Cosmology Cambridge, Madingley Road, Cambridge CB3 0HA, United Kingdom*

Received 2010 July 24; accepted 2010 August 16

Abstract. We present further observations of the Lockman Hole field, made with the Giant Metrewave Radio Telescope at 610 MHz with a resolution of $6{\times}5$ arcsec^2. These complement our earlier observations of the central $\approx$ 5 deg^2 by covering a further $\approx$ 8 deg^2, with an r.m.s. noise down to $\sim$ 80 μJy beam^{-1}. A catalogue of 4934 radio sources is presented.

Keywords : catalogues – surveys – radio continuum: galaxies

1. Introduction

The 'Lockman Hole' is a region of very low HI column density (Lockman, Jahoda & McCammon 1986) near $10^{\rm h}46^{\rm m}$, 58° (J2000.0), and is an ideal region for deep observations at X-ray wavelengths, due to low absorption. As a consequence the field has also become a standard field for deep observing campaigns in the optical, infrared and radio. Deep infrared observations are available for an area of $\approx$ 14 deg^2 of the Lockman Hole region as part of the Spitzer Wide-area Infrared Extragalactic (SWIRE) survey (Lonsdale et al. 2003). Parts of the Lockman Hole have also been observed in several deep X-rays surveys, including: (i) the Chandra Lockman Area North Survey (CLANS) and Chandra Large Area Synoptic X-Ray Survey (CLASXS), which cover $\approx$ 0.8 and 0.4 deg^2 centred near $10^{\rm h}46^{\rm m}$, 59°0′ and $10^{\rm h}34^{\rm m}$, 57°30′ respectively (Yang et al. 2004; Trouille et al. 2008; Wilkes et al. 2009) – and (ii) an XMM-Newton survey of $\approx$ 0.2 deg^2 centred near $10^{\rm h}52^{\rm m}$, 57°20′ (Hasinger et al. 2001; Brunner et al. 2008). Various radio observations have been

*deceased
†e-mail: D.A.Green@mrao.cam.ac.uk

made of portions of the Lockman Hole region, including very deep Very Large Array (VLA) and Giant Metrewave Radio Telescope (GMRT) radio surveys of parts of the CLANS, CLASXS and XMM-Newton X-rays survey regions (e.g. Ciliegi et al. 2003; Oyabu et al. 2005; Biggs & Ivison 2006, 2008; Owen & Morrison 2008; Owen et al. 2009; Ibar et al. 2009).

We have previously observed a central portion of the Lockman Hole field (Garn et al. 2008a, hereafter Paper I) at 610 MHz with the GMRT (see Rao 2002). These observations covered ≈ 5 deg^2 in the middle of the Lockman Hole, with twelve individual pointings, which overlapped portions of the Chandra CLANS and XMM-Newton X-ray fields. These observations had a resolution of 6×5 arcsec^2, at position angle (PA) +45°, with a typical r.m.s. noise of ~ 60 μJy beam^{-1} in the centre of the pointings. A catalogue of 2845 sources detected in the field was presented. These observations were part of a series of relatively deep, wide field observations of several SWIRE fields, and of the Spitzer Extragalactic First Look Survey region (see Garn et al. 2007, 2008b, 2009) .

Here we present further observations of the Lockman Hole field at 610 MHz with the GMRT. These observations are not as deep as those available for some areas of the Lockman Hole (see references above), but cover a further ≈ 8 deg^2, completing coverage of the Chandra CLANS and XMM-Newton X-fields, and also covering the CLASXS field. The observations and their data reduction are described in Section 2, and the results – including details of the catalogue of 4934 sources – are presented in Section 3.

2. Observations and data reduction

The GMRT is an interferometer consisting of thirty 45-m antennas, twelve of which are arranged within a central ≈ 1 km $\times$ 1 km region, and the others in three arms giving baselines up to about 30 km. We observed 26 pointings in the Lockman Hole region on a hexagonal grid surrounding the 12 pointings observed in Paper I (see Fig. 1). These pointings were initially observed on 2006 July 16 and 17, but the first day's observations suffered from power outage in the eastern arm of the GMRT. Consequently further observations were scheduled on September 7, 8 and 12, but again power problems led to loss of some observing time, and a final observation session was scheduled on October 4. In total, ≈ 21 hours of data, including calibration observations, were obtained. The observations were made with two 16-MHz sidebands centred on 610 MHz, each of which was split in 128 narrow channels, with both left and right circular polarisations.

The observations consisted of interleaved scans of the different pointings, typically ≈ 6 min in duration, and observations of the nearby compact calibrator source J1035+564 every 30 min or so. The flux density calibrators 3C48 or 3C286 were observed at the beginning and end of each observing session. The data from each observing session were calibrated and processed using similar procedures to those described in Paper I. In summary: obvious interference and other problematic data were flagged; the flux scale was tied to 3C48 or 3C286, with assumed flux densities of 29.4 and 21.1 Jy respectively at 610 MHz; the observations of 3C48 or 3C286 were used to characterise the bandpass response of each antenna; the amplitude and phase stability of

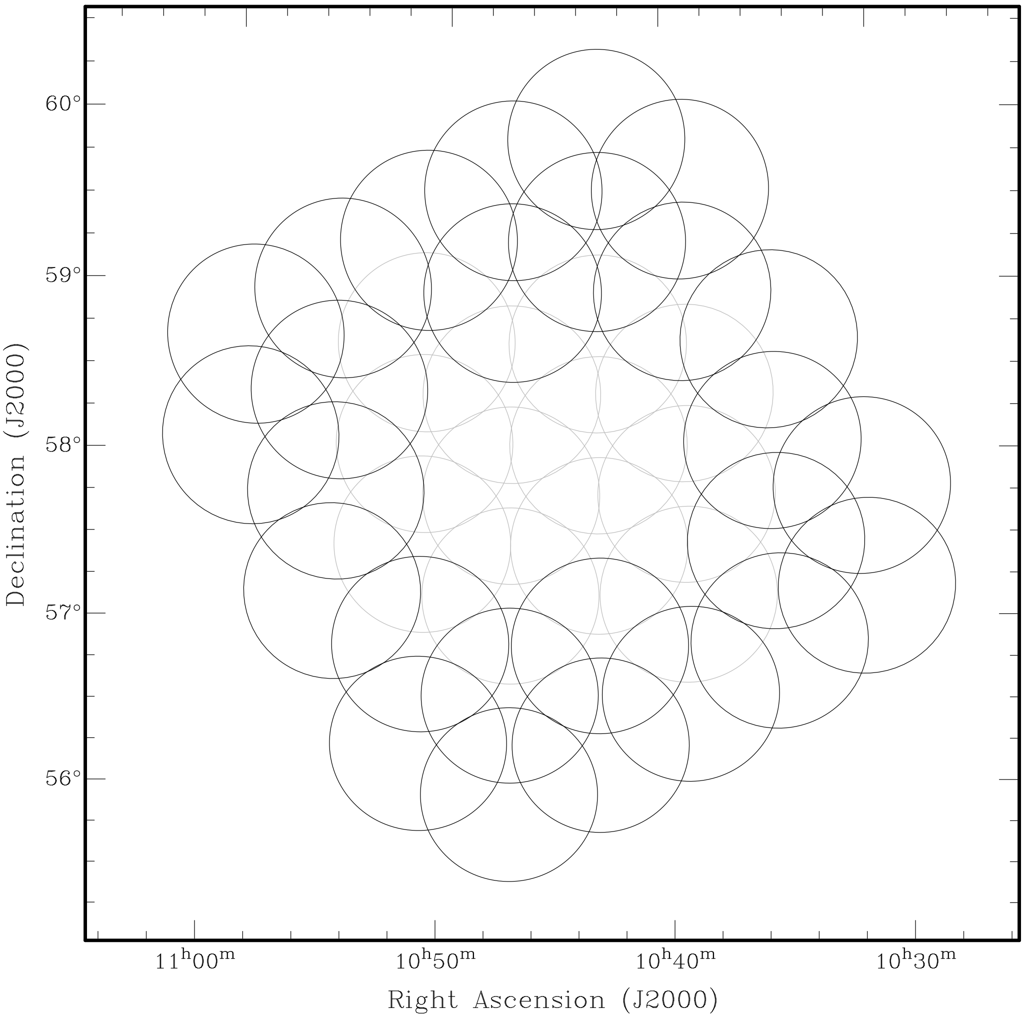

Figure 1. GMRT pointings in the Lockman Hole region, with circles indicating the primary beam HPBW (the results from the central 12 pointings – shown in grey – were presented in Paper I).

each antenna were calibrated from the short observations of J1035+564. After the calibrations were applied, the data were integrated into 11 channels of bandwidth 1.25 MHz, and some further flagging of bad data was made. The observations of each pointing, from all the different observation sessions, and both sidebands, were combined; typically each pointing was observed for 5 scans, i.e. a total of about 30 min. For each pointing Stokes *I* images were then synthesised using 31 smaller facets, arranged in a hexagonal grid. All images were synthesised with an elliptical restoring beam of size 6×5 arcsec^2, PA +45° (to match the images in Paper I), with a pixel size of 1.5 arcsec to ensure that the beam was well oversampled. The images went through three iterations of phase self-calibration at 10, 3 and 1 min intervals, and then a final iteration of phase and amplitude self-calibration, at 10 min intervals, with the overall amplitude gain held constant in order not to alter the flux density of sources. The self-calibration steps improved the noise level by about 10 per cent, and significantly reduced the residual sidelobes around the brighter sources. The final r.m.s. noise, before correction for the GMRT primary beam, varied considerably between pointings. In particular, in the west of the field there is the bright source 3C244.1 (see below), and the noise near this is increased, due to dynamic range limitations. (Indeed, in Paper I, the noise of the two northwestern inner pointings was also noted as being high, due to the proximity of these pointings to 3C244.1.) The noise in most of the pointings to the east is typically 80 μJy beam^{-1}, before primary beam correction. This is slightly higher than for the inner 12 pointings presented in Paper I, as expected due to the somewhat shorter integration time per pointing. The r.m.s. noise values in pointings in the west, particularly those close to 3C244.1 are considerably worse, by factors of up to about three. Both the inner and outer pointings were mosaicked together, with weighting appropriate to the relative noise of each pointing. The contribution to the mosaic was cut off at the point where the primary beam correction for each pointing dropped to 20 per cent, i.e. a radius of 32 arcmin from the centre of each pointings.

3. Results

The final mosaicked image is 13000×13000 pixel^2, so is difficult to display in its entirety. A sample region in the outer eastern portion of the image is presented in Fig. 2, to illustrate the quality of the imaging away from bright sources.

As noted above, in the western part of the Lockman Hole field there is the bright radio source 3C244.1 (e.g. Alexander & Leahy 1987; Gilbert et al. 2004), an extragalactic FR type II source (Fanaroff & Riley 1974) which is about 1 arcmin in extent, with an integrated flux density of ≈ 10.5 Jy at 610 MHz (Fig. 3).

A catalogue of radio sources was made in a way similar to that used in Paper I. An initial catalogue of sources within the 30 per cent primary response with a peak brightness of greater than six times the local noise was made using SExtractor (Bertin & Arnouts 1996). Using the technique described in Garn et al. (2008b), close to brighter (> 10 mJy peak) sources a more stringent cutoff of at least 12 times the local noise was applied. Table 1 presents a sample of 163 sources from the catalogue, in the region $10^{\mathrm{h}}30^{\mathrm{m}}50^{\mathrm{s}}$ to $10^{\mathrm{h}}36^{\mathrm{m}}20^{\mathrm{s}}$, $+57°18'$ to $58°06'$, i.e. the region covered by the CLASXS X-ray survey. Column 1 gives the IAU designation of the source, in the form GMRTLH Jhhmmss.s+ddmmss, where J represents J2000.0 coordinates, hhmmss.s represents RA in hours, minutes and truncated tenths of seconds and ddmmss represents the Dec in degrees, arcminutes and truncated arcseconds. Columns 2 and 3 give the RA and Dec of the source, calculated using first moments of the relevant pixel brightnesses to give a centroid position. Column 4 gives the brightness of the peak pixel in each source, S_{peak}, in mJy beam^{-1}, and Column 5 gives the local r.m.s. noise, σ, in μJy beam^{-1}. Columns 6 and 7 give the integrated flux density and error, S_{int} and ΔS_{int}, in mJy. Columns 8 and 9 give the X, Y pixel coordinates from the mosaic image of the source centroid. Column 10 is the SExtractor deblended object

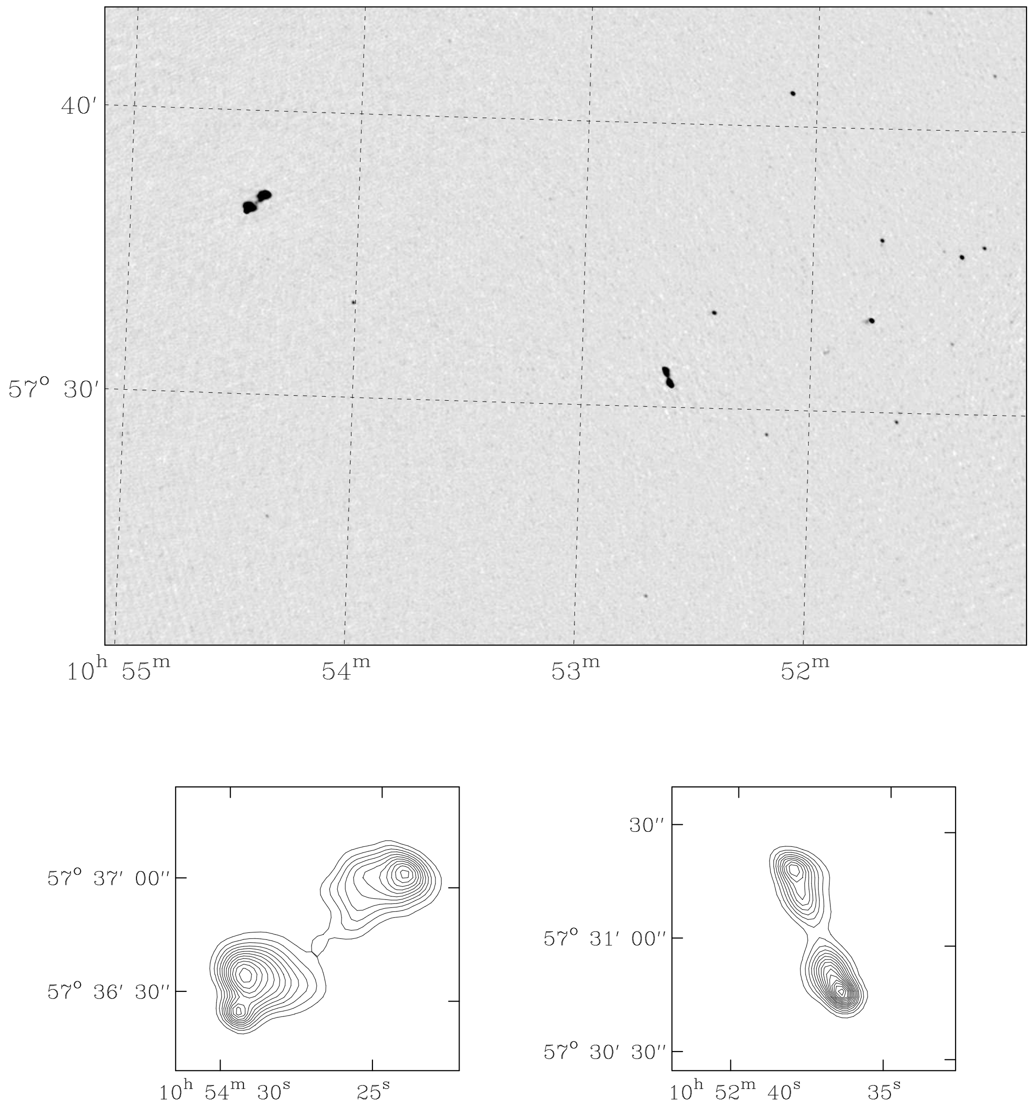

Figure 2. A sample 610-MHz greyscale image (from −0.5 to 4 mJy beam^{-1}), for an eastern outer portion of the Lockman Hole, with contour images for two brighter double sources in the field (contour levels equally spaced, every 2 mJy beam^{-1}). The resolution is 6×5 arcsec^2, at a PA +45°.

flag: (1) where a nearby bright source may be affecting the calculated flux, (2) where a source has been deblended into two or more components from a single initial island of flux and (3) where both of the above criteria apply. The final mosaic should be examined to check the cases where one extended object has been represented by two or more entries. Also, because of the limited

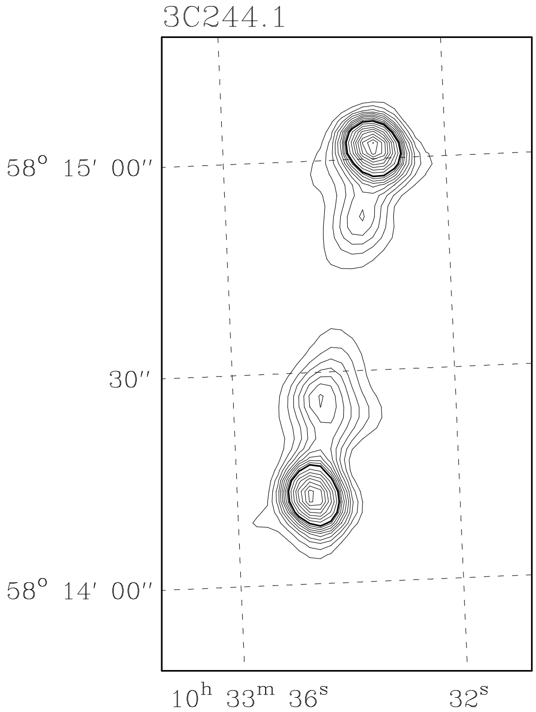

Figure 3. 610-MHz image of 3C244.1 from these observations. The contours are 0.1, 0.2, 0.3… 1.0, 1.2, 1.4… 2.8 Jy beam^{-1}. The resolution is 6×5 arcsec^2, at a PA +45°.

dynamic range of the GMRT, the parameters of sources near bright sources should be treated with some caution.

The final mosaicked image and the catalogue of 4934 sources are both available online from `http://www.mrao.cam.ac.uk/surveys/`, along with the results of our other GMRT surveys of various SWIRE fields and the Spitzer Extragalactic First Look Survey region.

Acknowledgements

We thank the staff of the GMRT who made these observations possible. In particular we thank Nimisha Kantharia for making the re-scheduled observations. The GMRT is run by the National Centre for Radio Astrophysics of the Tata Institute of Fundamental Research.

References

Alexander P., Leahy J. P., 1987, MNRAS, 225, 1
Bertin E., Arnouts S., 1996, A&AS, 117, 393
Biggs A. D., Ivison R. J., 2006, MNRAS, 371, 963
Biggs A. D., Ivison R. J., 2008, MNRAS, 385, 893

Brunner H., Cappelluti N., Hasinger G., Barcons X., Fabian A. C., Mainieri V., Szokoly G., 2008, A&A, 479, 283
Ciliegi P., Zamorani G., Hasinger G., Lehmann I., Szokoly G., Wilson G., 2003, A&A, 398, 901
Fanaroff B. L., Riley J. M., 1974, MNRAS, 167, 31P
Garn T., Green D. A., Hales S. E. G., Riley J. M., Alexander P., 2007, MNRAS, 376, 1251
Garn T., Green D. A., Riley J. M., Alexander P., 2008a, MNRAS, 387, 1037 (Paper I)
Garn T., Green D. A., Riley J. M., Alexander P., 2008b, MNRAS, 383, 75
Garn T., Green D. A., Riley J. M., Alexander P., 2009, MNRAS, 397, 1101
Gilbert G. M., Riley J. M., Hardcastle M. J., Croston J. H., Pooley G. G., Alexander P., 2004, MNRAS, 351, 845
Hasinger G., et al., 2001, A&A, 365, L45
Ibar E., Ivison R. J., Biggs A. D., Lal D. V., Best P. N., Green D. A., 2009, MNRAS, 397, 281
Lockman F. J., Jahoda K., McCammon D., 1986, ApJ, 302, 432
Lonsdale C. J., et al., 2003, PASP, 115, 897
Owen F. N., Morrison G. E., 2008, AJ, 136, 1889
Owen F. N., Morrison G. E., Klimek M. D., Greisen E. W., 2009, AJ, 137, 4846
Oyabu S., et al., 2005, AJ, 130, 2019
Rao A. P., 2002, IAUS, 199, 439
Trouille L., Barger A. J., Cowie L. L., Yang Y., Mushotzky R. F., 2008, ApJS, 179, 1
Wilkes B. J., et al., 2009, ApJS, 185, 433
Yang Y., Mushotzky R. F., Steffen A. T., Barger A. J., Cowie L. L., 2004, AJ, 128, 1501

Table 1: A sample of entries from the catalogue of radio sources in the Lockman Hole region. See text for details. These are sources in the CLASXS region.

Name (1)	RA (J2000.0) (2)	Dec (3)	S_{peak} (4)	σ (5)	S_{int} (6)	ΔS_{int} (7)	X (8)	Y (9)	flags (10)
GMRTLH J103050.9+574657	10:30:50.99	+57:46:57.0	0.874	140	1.043	0.126	11023	6097	0
GMRTLH J103055.6+572316	10:30:55.60	+57:23:16.2	0.626	96	0.651	0.090	11048	5150	0
GMRTLH J103055.8+575948	10:30:55.82	+57:59:48.9	14.804	154	19.687	0.330	10971	6610	0
GMRTLH J103059.3+572303	10:30:59.39	+57:23:03.8	3.755	101	4.181	0.183	11028	5141	0
GMRTLH J103102.6+573805	10:31:02.65	+57:38:05.6	1.591	121	1.466	0.143	10979	5740	0
GMRTLH J103105.0+575354	10:31:05.08	+57:53:54.3	99.348	438	117.786	1.099	10934	6371	0
GMRTLH J103113.3+572242	10:31:13.30	+57:22:42.2	0.552	87	0.969	0.100	10953	5122	0
GMRTLH J103118.5+574731	10:31:18.54	+57:47:31.7	0.983	157	0.824	0.135	10875	6113	0
GMRTLH J103118.7+574758	10:31:18.78	+57:47:58.0	1.129	160	0.972	0.185	10873	6130	0
GMRTLH J103120.3+571833	10:31:20.32	+57:18:33.8	0.746	103	0.626	0.100	10924	4955	0
GMRTLH J103122.3+580211	10:31:22.31	+58:02:11.7	1.087	150	2.705	0.229	10826	6697	0
GMRTLH J103123.0+574227	10:31:23.09	+57:42:27.3	1.171	117	0.916	0.124	10861	5909	0
GMRTLH J103123.4+580559	10:31:23.46	+58:05:59.3	1.201	192	2.040	0.198	10812	6849	0
GMRTLH J103126.1+573242	10:31:26.12	+57:32:42.6	0.813	103	0.553	0.089	10864	5519	0
GMRTLH J103126.9+572328	10:31:26.94	+57:23:28.7	0.504	80	0.392	0.069	10878	5149	0
GMRTLH J103129.5+572511	10:31:29.59	+57:25:11.3	4.884	94	8.831	0.205	10861	5217	0
GMRTLH J103130.4+580340	10:31:30.43	+58:03:40.3	1.109	165	3.122	0.262	10780	6754	0
GMRTLH J103131.2+573934	10:31:31.27	+57:39:34.1	4.718	118	5.069	0.193	10823	5791	0
GMRTLH J103133.5+572040	10:31:33.53	+57:20:40.6	0.702	90	0.518	0.081	10849	5036	0
GMRTLH J103134.3+574224	10:31:34.36	+57:42:24.2	1.774	116	1.668	0.166	10801	5904	0
GMRTLH J103136.2+580024	10:31:36.27	+58:00:24.1	1.240	163	2.901	0.238	10755	6622	0
GMRTLH J103138.3+575836	10:31:38.36	+57:58:36.1	0.908	149	1.548	0.184	10748	6550	0
GMRTLH J103138.6+572625	10:31:38.64	+57:26:25.6	5.531	92	5.861	0.157	10810	5264	0
GMRTLH J103141.8+580131	10:31:41.80	+58:01:31.2	1.374	150	1.949	0.229	10724	6665	0
GMRTLH J103155.2+580518	10:31:55.25	+58:05:18.4	1.463	205	2.919	0.265	10646	6813	0
GMRTLH J103156.2+580000	10:31:56.20	+58:00:00.5	1.006	145	1.424	0.180	10651	6601	0
GMRTLH J103156.6+573845	10:31:56.62	+57:38:45.6	1.741	104	1.704	0.140	10689	5752	0
GMRTLH J103157.0+580148	10:31:57.07	+58:01:48.5	1.400	185	2.904	0.270	10643	6673	0
GMRTLH J103157.8+580137	10:31:57.80	+58:01:37.5	1.155	190	1.775	0.203	10639	6665	0
GMRTLH J103200.3+580043	10:32:00.38	+58:00:43.7	1.212	170	1.326	0.164	10627	6629	0
GMRTLH J103200.9+574944	10:32:00.95	+57:49:44.3	19.057	181	20.071	0.370	10645	6190	0
GMRTLH J103201.4+580115	10:32:01.40	+58:01:15.1	1.370	183	1.758	0.217	10621	6650	0
GMRTLH J103204.9+575309	10:32:04.94	+57:53:09.1	0.982	149	1.444	0.180	10618	6325	0
GMRTLH J103207.6+572153	10:32:07.61	+57:21:53.5	12.099	92	12.863	0.192	10663	5075	0
GMRTLH J103210.7+571821	10:32:10.71	+57:18:21.5	1.583	82	1.442	0.108	10653	4933	0
GMRTLH J103215.6+580208	10:32:15.66	+58:02:08.5	1.129	176	1.425	0.223	10544	6682	0
GMRTLH J103216.7+575435	10:32:16.72	+57:54:35.4	1.052	157	1.087	0.151	10552	6380	0
GMRTLH J103220.1+575833	10:32:20.16	+57:58:33.8	1.228	174	1.881	0.195	10527	6537	0
GMRTLH J103220.7+573835	10:32:20.72	+57:38:35.0	3.483	102	3.837	0.163	10561	5739	0
GMRTLH J103221.7+573819	10:32:21.76	+57:38:19.2	0.677	102	0.669	0.095	10556	5728	0
GMRTLH J103222.6+580234	10:32:22.63	+58:02:34.4	1.499	242	3.274	0.265	10506	6697	0
GMRTLH J103222.8+575550	10:32:22.85	+57:55:50.0	9.548	166	16.004	0.397	10518	6428	0
GMRTLH J103235.7+571859	10:32:35.72	+57:18:59.6	0.547	83	0.464	0.071	10517	4953	0
GMRTLH J103238.3+572220	10:32:38.33	+57:22:20.8	0.639	89	0.538	0.077	10496	5086	0
GMRTLH J103239.2+580046	10:32:39.29	+58:00:46.2	1.317	216	2.256	0.262	10421	6621	0
GMRTLH J103239.8+574611	10:32:39.83	+57:46:11.7	1.073	131	0.909	0.136	10445	6038	0
GMRTLH J103241.6+573010	10:32:41.60	+57:30:10.5	2.310	93	2.541	0.143	10465	5398	0
GMRTLH J103241.6+580120	10:32:41.68	+58:01:20.1	1.748	187	3.818	0.338	10408	6643	0
GMRTLH J103243.2+571809	10:32:43.29	+57:18:09.0	0.509	79	0.366	0.064	10477	4917	0
GMRTLH J103243.2+580029	10:32:43.24	+58:00:29.1	1.395	212	1.899	0.290	10401	6609	0
GMRTLH J103252.5+573115	10:32:52.55	+57:31:15.5	7.251	108	11.178	0.242	10404	5438	3
GMRTLH J103254.6+573124	10:32:54.68	+57:31:24.7	11.001	102	14.394	0.230	10392	5444	3
GMRTLH J103259.8+575321	10:32:59.86	+57:53:21.1	1.501	126	1.276	0.142	10326	6320	0

Name (1)	RA (J2000.0) (2)	Dec (3)	$S_{\rm peak}$ (4)	σ (5)	$S_{\rm int}$ (6)	$\Delta S_{\rm int}$ (7)	X (8)	Y (9)	flags (10)
GMRTLH J103303.3+575517	10:33:03.39	+57:55:17.7	1.096	139	6.331	0.320	10304	6396	0
GMRTLH J103305.9+573502	10:33:05.92	+57:35:02.5	0.702	103	0.503	0.084	10326	5587	0
GMRTLH J103311.1+574208	10:33:11.16	+57:42:08.4	1.035	103	1.898	0.153	10285	5869	3
GMRTLH J103312.3+574217	10:33:12.35	+57:42:17.1	1.278	102	2.416	0.178	10279	5874	2
GMRTLH J103314.5+573935	10:33:14.51	+57:39:35.0	3.740	104	5.446	0.205	10272	5766	3
GMRTLH J103314.6+573920	10:33:14.61	+57:39:20.6	6.056	103	7.879	0.204	10272	5756	3
GMRTLH J103315.5+573101	10:33:15.56	+57:31:01.9	0.763	91	0.720	0.097	10281	5424	0
GMRTLH J103317.3+572718	10:33:17.39	+57:27:18.6	0.581	82	0.386	0.070	10278	5275	0
GMRTLH J103324.8+575931	10:33:24.85	+57:59:31.5	1.116	177	1.692	0.228	10182	6561	0
GMRTLH J103328.1+573241	10:33:28.19	+57:32:41.3	0.619	85	0.586	0.080	10210	5487	0
GMRTLH J103332.7+580012	10:33:32.75	+58:00:12.2	1.218	179	1.912	0.212	10139	6586	1
GMRTLH J103332.9+580028	10:33:32.94	+58:00:28.2	1.104	181	3.657	0.264	10138	6596	0
GMRTLH J103333.8+575947	10:33:33.82	+57:59:47.3	1.427	184	1.937	0.222	10135	6569	0
GMRTLH J103334.1+573201	10:33:34.18	+57:32:01.0	0.504	81	0.680	0.076	10179	5459	0
GMRTLH J103343.2+572549	10:33:43.29	+57:25:49.7	0.530	82	0.413	0.067	10141	5210	0
GMRTLH J103344.6+573332	10:33:44.60	+57:33:32.6	0.528	79	0.337	0.061	10121	5518	0
GMRTLH J103345.9+574013	10:33:45.99	+57:40:13.0	0.540	84	0.524	0.069	10103	5784	0
GMRTLH J103346.6+575504	10:33:46.64	+57:55:04.1	0.766	126	0.758	0.098	10074	6378	0
GMRTLH J103347.0+574945	10:33:47.02	+57:49:45.9	0.721	103	0.635	0.084	10081	6166	0
GMRTLH J103357.7+573653	10:33:57.73	+57:36:53.9	1.108	95	0.787	0.099	10045	5649	0
GMRTLH J103358.7+574316	10:33:58.76	+57:43:16.2	2.082	90	2.152	0.134	10029	5903	0
GMRTLH J103359.2+572951	10:33:59.20	+57:29:51.6	2.956	76	3.249	0.137	10049	5367	0
GMRTLH J103405.4+573329	10:34:05.42	+57:33:29.1	0.477	70	0.910	0.076	10010	5511	0
GMRTLH J103408.5+573702	10:34:08.52	+57:37:02.3	0.598	83	0.513	0.075	9987	5652	0
GMRTLH J103411.5+575528	10:34:11.50	+57:55:28.5	0.887	145	0.917	0.145	9942	6388	0
GMRTLH J103414.9+573219	10:34:14.91	+57:32:19.9	0.530	82	0.736	0.082	9961	5463	0
GMRTLH J103415.4+573408	10:34:15.41	+57:34:08.1	1.546	75	1.695	0.126	9955	5535	0
GMRTLH J103419.7+574203	10:34:19.72	+57:42:03.5	0.585	91	1.057	0.115	9919	5850	0
GMRTLH J103422.4+574207	10:34:22.46	+57:42:07.9	1.277	103	3.926	0.226	9905	5853	0
GMRTLH J103423.5+572136	10:34:23.54	+57:21:36.0	1.099	79	1.073	0.096	9931	5032	0
GMRTLH J103425.5+574212	10:34:25.55	+57:42:12.8	0.855	102	1.289	0.126	9888	5855	0
GMRTLH J103426.7+574254	10:34:26.76	+57:42:54.6	0.653	90	0.597	0.080	9881	5883	0
GMRTLH J103433.3+573146	10:34:33.33	+57:31:46.6	0.847	70	0.894	0.085	9863	5437	0
GMRTLH J103434.1+572910	10:34:34.17	+57:29:10.5	0.814	76	1.005	0.107	9862	5332	0
GMRTLH J103435.6+572759	10:34:35.68	+57:27:59.6	1.395	84	1.520	0.117	9856	5285	0
GMRTLH J103436.3+575048	10:34:36.32	+57:50:48.7	0.817	105	0.595	0.090	9817	6197	0
GMRTLH J103446.9+573105	10:34:46.97	+57:31:05.6	0.568	91	0.321	0.062	9791	5407	0
GMRTLH J103450.3+573949	10:34:50.33	+57:39:49.4	0.994	84	0.748	0.090	9759	5755	0
GMRTLH J103452.7+580441	10:34:52.74	+58:04:41.0	1.702	261	2.359	0.243	9709	6748	0
GMRTLH J103452.9+580426	10:34:52.90	+58:04:26.6	1.630	253	5.148	0.326	9709	6738	0
GMRTLH J103453.7+575405	10:34:53.79	+57:54:05.2	0.730	117	0.615	0.101	9720	6324	0
GMRTLH J103454.1+580507	10:34:54.19	+58:05:07.9	2.380	327	3.529	0.413	9701	6766	0
GMRTLH J103454.7+573318	10:34:54.75	+57:33:18.9	0.979	120	1.283	0.139	9746	5494	0
GMRTLH J103455.2+574518	10:34:55.28	+57:45:18.1	0.561	90	0.488	0.087	9725	5973	0
GMRTLH J103457.1+580517	10:34:57.10	+58:05:17.2	3.392	326	8.473	0.588	9685	6771	0
GMRTLH J103457.2+580253	10:34:57.21	+58:02:53.1	1.464	190	3.343	0.306	9688	6675	0
GMRTLH J103457.9+573941	10:34:57.92	+57:39:41.3	0.626	85	0.707	0.082	9719	5748	0
GMRTLH J103459.4+573256	10:34:59.49	+57:32:56.9	0.807	115	0.508	0.089	9721	5478	0
GMRTLH J103500.2+580458	10:35:00.26	+58:04:58.7	1.850	241	2.477	0.278	9669	6758	0
GMRTLH J103501.2+573317	10:35:01.28	+57:33:17.8	0.811	128	0.823	0.105	9711	5492	0
GMRTLH J103501.7+571930	10:35:01.70	+57:19:30.8	0.495	78	0.378	0.064	9728	4941	0
GMRTLH J103502.3+572341	10:35:02.36	+57:23:41.2	11.880	98	12.775	0.204	9719	5107	0
GMRTLH J103504.0+573128	10:35:04.02	+57:31:28.0	0.858	137	0.790	0.112	9699	5418	0
GMRTLH J103505.1+575821	10:35:05.15	+57:58:21.5	1.039	166	1.020	0.142	9653	6493	0
GMRTLH J103505.7+572737	10:35:05.79	+57:27:37.8	1.712	78	1.991	0.125	9695	5264	0
GMRTLH J103505.9+573030	10:35:05.92	+57:30:30.1	0.694	111	0.537	0.091	9690	5379	0
GMRTLH J103506.0+580422	10:35:06.02	+58:04:22.8	1.639	250	2.120	0.274	9640	6733	0

Name	RA (J2000.0)	Dec	$S_{\rm peak}$	σ	$S_{\rm int}$	$\Delta S_{\rm int}$	X	Y	flags
(1)	(2)	(3)	(4)	(5)	(6)	(7)	(8)	(9)	(10)
GMRTLH J103507.9+574227	10:35:07.94	+57:42:27.6	0.524	81	0.468	0.067	9662	5857	0
GMRTLH J103508.0+580409	10:35:08.04	+58:04:09.7	2.457	265	4.767	0.415	9629	6724	0
GMRTLH J103508.8+573737	10:35:08.88	+57:37:37.7	1.449	92	1.175	0.109	9664	5663	0
GMRTLH J103509.2+573302	10:35:09.29	+57:33:02.9	0.949	155	0.684	0.120	9668	5480	0
GMRTLH J103509.7+580230	10:35:09.77	+58:02:30.4	1.486	222	1.532	0.214	9623	6658	2
GMRTLH J103510.2+580444	10:35:10.26	+58:04:44.8	2.572	263	3.638	0.352	9617	6747	0
GMRTLH J103511.3+573403	10:35:11.38	+57:34:03.4	0.906	139	1.260	0.175	9655	5520	0
GMRTLH J103511.5+580307	10:35:11.55	+58:03:07.4	1.700	213	1.996	0.246	9612	6682	0
GMRTLH J103511.8+573222	10:35:11.85	+57:32:22.9	0.926	150	0.871	0.129	9655	5453	0
GMRTLH J103512.2+573125	10:35:12.25	+57:31:25.5	1.018	148	0.732	0.121	9654	5415	0
GMRTLH J103512.8+574001	10:35:12.83	+57:40:01.4	0.602	80	0.581	0.077	9639	5758	0
GMRTLH J103513.4+580547	10:35:13.46	+58:05:47.9	3.714	455	19.052	1.124	9598	6789	0
GMRTLH J103513.7+580454	10:35:13.79	+58:04:54.0	1.851	278	1.657	0.238	9598	6753	0
GMRTLH J103513.9+574249	10:35:13.93	+57:42:49.8	0.706	83	0.533	0.080	9629	5870	0
GMRTLH J103514.6+573142	10:35:14.62	+57:31:42.3	1.044	151	0.955	0.123	9641	5426	0
GMRTLH J103516.2+580146	10:35:16.25	+58:01:46.9	1.744	213	3.388	0.330	9589	6627	0
GMRTLH J103516.5+580057	10:35:16.51	+58:00:57.5	0.980	157	2.729	0.190	9589	6594	0
GMRTLH J103517.9+580517	10:35:17.91	+58:05:17.8	2.337	346	6.311	0.564	9576	6768	0
GMRTLH J103520.6+580123	10:35:20.61	+58:01:23.1	1.335	197	1.829	0.209	9567	6611	3
GMRTLH J103521.5+574840	10:35:21.50	+57:48:40.3	0.529	86	0.392	0.071	9580	6102	0
GMRTLH J103522.1+573720	10:35:22.14	+57:37:20.0	1.997	96	2.099	0.136	9593	5649	0
GMRTLH J103523.2+573900	10:35:23.24	+57:39:00.1	4.368	85	4.407	0.143	9585	5715	0
GMRTLH J103523.3+573247	10:35:23.32	+57:32:47.7	3.619	128	8.312	0.307	9593	5467	0
GMRTLH J103524.0+573526	10:35:24.06	+57:35:26.7	0.655	95	0.513	0.081	9585	5573	0
GMRTLH J103526.9+573035	10:35:26.90	+57:30:35.2	2.264	129	2.555	0.183	9577	5378	0
GMRTLH J103528.3+580320	10:35:28.37	+58:03:20.3	1.534	249	3.334	0.301	9523	6687	0
GMRTLH J103529.2+572925	10:35:29.28	+57:29:25.5	0.694	101	0.487	0.078	9566	5332	0
GMRTLH J103530.3+575216	10:35:30.38	+57:52:16.9	0.867	115	1.175	0.130	9528	6245	0
GMRTLH J103533.0+573259	10:35:33.08	+57:32:59.8	0.821	118	0.520	0.091	9540	5474	0
GMRTLH J103534.6+572814	10:35:34.62	+57:28:14.6	0.631	99	0.579	0.089	9539	5283	0
GMRTLH J103536.8+573329	10:35:36.89	+57:33:29.2	0.694	110	1.010	0.114	9519	5492	0
GMRTLH J103540.1+573324	10:35:40.19	+57:33:24.5	0.871	102	1.413	0.150	9502	5489	0
GMRTLH J103540.5+575529	10:35:40.56	+57:55:29.7	0.746	123	1.067	0.114	9469	6372	0
GMRTLH J103541.3+575622	10:35:41.35	+57:56:22.1	0.816	132	1.385	0.132	9464	6406	0
GMRTLH J103541.9+580415	10:35:41.94	+58:04:15.6	1.026	162	1.833	0.217	9450	6722	0
GMRTLH J103542.3+580441	10:35:42.30	+58:04:41.4	1.077	163	1.004	0.140	9448	6739	0
GMRTLH J103544.8+573206	10:35:44.81	+57:32:06.9	0.681	88	0.714	0.097	9479	5436	3
GMRTLH J103546.1+574310	10:35:46.16	+57:43:10.4	0.818	82	0.938	0.093	9457	5878	0
GMRTLH J103550.4+573629	10:35:50.48	+57:36:29.8	0.648	91	0.578	0.078	9442	5610	0
GMRTLH J103550.6+573257	10:35:50.67	+57:32:57.5	0.569	85	0.624	0.085	9446	5469	0
GMRTLH J103554.3+574642	10:35:54.30	+57:46:42.0	0.556	88	0.488	0.072	9408	6018	0
GMRTLH J103557.4+573517	10:35:57.43	+57:35:17.3	0.770	77	0.611	0.099	9407	5561	0
GMRTLH J103559.1+572429	10:35:59.16	+57:24:29.9	0.515	85	0.650	0.090	9412	5129	0
GMRTLH J103600.8+580048	10:36:00.88	+58:00:48.3	1.132	185	3.704	0.294	9355	6580	0
GMRTLH J103607.3+575106	10:36:07.33	+57:51:06.0	3.120	132	3.661	0.221	9333	6191	0
GMRTLH J103609.2+573245	10:36:09.25	+57:32:45.6	0.624	85	0.941	0.094	9347	5458	0
GMRTLH J103610.0+575115	10:36:10.00	+57:51:15.8	18.114	137	25.505	0.343	9319	6197	0
GMRTLH J103610.4+573134	10:36:10.42	+57:31:34.7	0.516	83	0.479	0.077	9342	5410	0
GMRTLH J103611.8+572524	10:36:11.87	+57:25:24.3	0.529	83	0.738	0.080	9342	5163	0
GMRTLH J103613.6+574004	10:36:13.69	+57:40:04.7	0.553	83	0.597	0.081	9314	5749	0
GMRTLH J103614.4+572346	10:36:14.46	+57:23:46.9	0.593	85	0.703	0.076	9331	5098	0
GMRTLH J103614.4+573554	10:36:14.41	+57:35:54.3	0.633	95	0.417	0.074	9315	5582	0
GMRTLH J103617.6+572617	10:36:17.68	+57:26:17.3	0.630	87	0.981	0.096	9310	5197	0

Dr Timothy S. Garn (1982–2010)

The paper 'Further GMRT observations of the Lockman Hole at 610 MHz' describes some deep, wide-field observations made with the Giant Metrewave Radio Telescope (GMRT). We would like to dedicate this to the memory of the first author, Timothy Garn, who died earlier this year.

Tim studied as an undergraduate at Christ's College in the University of Cambridge UK from October 2001. He graduated with BA and MSci degrees in June 2005, having obtained very good firsts in the University examinations in each of his four undergraduate years. He stayed in Cambridge for his PhD studies, working in the Astrophysics Group in the Cavendish Laboratory on deep, wide-field 610-MHz surveys made with the GMRT. He started his PhD in October 2005 and, exceptionally, in just under three years he had completed an excellent PhD thesis; during this time he also produced a number of papers based on the observations made with the GMRT, and on comparisons of the radio results with other data. In September 2008 Tim moved to a postdoctoral research position at the Royal Observatory, Edinburgh, where he quickly extended his research into new areas, relating in particular to the development of LOFAR.

Sadly Tim died in January 2010, in a mountaineering accident on Ben Lui in Scotland.

During his PhD studies, Tim showed great promise as an observational astronomer. He quickly learned new skills, and applied them to the challenges raised by his studies. His careful analysis of the deep, wide-field observations made with the GMRT at 610 MHz provided not only high-quality scientific results, but also helped identify and resolve problems with the instrument, which allowed others to make better observations. Tim was a confident, very capable and accomplished scientist, and it was a pleasure to work with him.

The paper on further GMRT observations of the Lockman Hole, published in this issue, is the final part of the observational work carried out by Tim for his thesis; he completed the analysis of the data last year after leaving Cambridge. We have prepared this work for publication as a tribute to Tim.

Paul Alexander, Dave Green, Julia Riley
Astrophysics Group, Cavendish Laboratory, Cambridge, UK